

Constraints on the Dark Matter Annihilations by Neutrinos with Substructure Effects Included

Peng-fei Yin ¹, Jia Liu ¹, Qiang Yuan ³, Xiao-jun Bi ^{2,3} and Shou-hua Zhu ¹

¹ *Institute of Theoretical Physics & State Key Laboratory of Nuclear Physics and Technology, Peking University, Beijing 100871, China*

² *Center for High Energy Physics, Peking University, Beijing 100871, China*

³ *Key Laboratory of Particle Astrophysics, Institute of High Energy Physics, Chinese Academy of Sciences, Beijing 100049, P. R. China*

(Dated: July 27, 2021)

Dark matter (DM) annihilations in the Galaxy may produce high energy neutrinos, which can be detected by the neutrino telescopes, for example IceCube, ANTARES and Super-Kamiokande. The neutrinos can also arise from hadronic interaction between cosmic ray and atmosphere around the Earth, known as atmospheric neutrino. Current measurements on neutrino flux is consistent with theoretical prediction of atmospheric neutrino within the uncertainties. In this paper, by requiring that the DM annihilation neutrino flux is less than the current measurements, we obtain an upper bound on the cross section of dark matter annihilation $\langle\sigma v\rangle$. Compared with previous investigations, we improve the bound by including DM substructure contributions. In our paper, two kinds of substructure effects are scrutinized. One is the substructure average contribution over all directions. The other is point source effect by single massive sub-halo. We found that the former can improve the bound by several times, while the latter can improve the bound by $10^1 \sim 10^4$ utilizing the excellent angular resolution of neutrino telescope IceCube. The exact improvement depends on the DM profile and the sub-halo concentration model. In some model, IceCube can achieve the sensitivity of $\langle\sigma v\rangle \sim 10^{-26} \text{cm}^3 \text{s}^{-1}$.

PACS numbers: 13.15.+g, 95.35.+d, 95.55.Vj, 98.62.Gq

I. INTRODUCTION

Many astronomical observations indicate that most of the matter in our universe is dark (see e.g. Ref. [1]). The evidences come mainly from the gravitational effects of the dark matter (DM), such as the rotation curves of spiral galaxies [2, 3], the gravitational lensing [4] and the dynamics of galaxy clusters [5]. The studies such as primordial nucleosynthesis [6] and cosmic microwave background (CMB) [7] show that the DM is mostly non-baryonic. Combining recent cosmological measurements, for example from the Wilkinson Microwave Anisotropy Probe (WMAP), one could deduce precisely the relic density of DM, namely $\Omega_{DM}h^2 = 0.1143 \pm 0.0034$ [8]. However, the nature of dark matter is still unclear. In the literature there is a “zoo” of particle candidates for DM [9], among which the most popular candidate at present is the weakly interacting massive particle (WIMP) such as the lightest supersymmetric particle (LSP), lightest Kaluza-Klein particle (LKP) *etc.*

Search for WIMP in particle physics experiments is very important to pin down the properties of the DM. Besides searching missing energy signals at accelerator-based experiments, there are usually two classes of methods to detect WIMP, namely direct and indirect ones. The former method detects WIMP by measuring the recoil of heavy nucleus in the detector and gives the most strong evidence for the existence of DM. The latter one detects the DM self-annihilation signals, which include neutrinos, photons, anti-matter particles and so on. Among them neutrinos are one of the most attractive signals. For the *low energy* neutrinos (say much less than 100 GeV), their interactions with matter are highly suppressed by a factor at least Q^2/m_W^2 with Q the typical energy scale of the interaction. The neutrinos are hardly energy loss and trajectory deflection during their propagation, therefore they may carry the information of the nature and distribution of the DM. However due to the same reason, it is hard to capture such kind of *low energy* and relatively low flux neutrinos. For the *high energy* neutrinos (say around 100 GeV or higher), the interactions among neutrinos and matter become much stronger. These neutrinos may keep the information of the DM, and it is relatively easy to observe them experimentally.

One proposal of detecting the high energy neutrino signals is to explore the locations close to us such as the center of the Sun or the Earth to get enough neutrino flux. The DM particles are gravitational trapped in the center of the Sun or Earth and produce neutrinos by annihilation [10]. If the annihilation and capture processes are in equilibrium, the neutrino

flux are mainly determined by the cross section of the DM and nuclei. Another proposal is to detect the neutrino signals from DM annihilation in the Milky Way (MW). Though the sources in the MW are farther than the Sun, it is natural to expect that the larger amount of DM can compensate the distance. Moreover the neutrino flux depends on the DM annihilation rate and number density square, therefore the regions with high density in the MW, such as the Galactic Center (GC) or sub-halos, should be potentially excellent observational targets.

The GC is conventionally thought to be source-rich astrophysical laboratory and has attracted many attention of astronomers. It is also true for the DM indirect searches. Due to the weak interaction of DM particles, the DM density at the GC is highly accumulated as shown by detail simulations, which makes the GC a bright source of DM annihilation. However, the complicated astrophysical environment and various kinds of astrophysical sources make the GC a high background site. In addition, the overlapping with baryonic matter objects (e.g., the central massive black hole [11]) may also affect the DM distribution and increase the uncertainties. It should be emphasized that the galactic sub-halos may be good candidates as DM sources. Since the self-annihilation of DM is square-dependent on the number density, the clump of substructure is expected to effectively enhance the annihilation signal and plays a role of the so-called “boost factor” [12, 13, 14]. Furthermore as indicated by simulations, the spatial distribution of DM sub-halos is tend to be spherical symmetric in the MW halo, which may locate at a low-background site and effectively avoid the source confusion in the galactic plane. The effects of DM sub-halos on the flux of induced neutrino is what we try to investigate in this work.

The neutrinos detected by high-energy neutrino telescopes such as Super-Kamikande [15], AMANDA [16] etc. are thought to be mainly from atmospheric neutrinos. Here they originate from the decay of hadrons which are produced by the strong interactions of cosmic rays with atmosphere. Experimentally no obvious excess has yet been observed. Then the measurements on neutrino flux can be utilized to set bounds on the DM annihilation cross section. As neutrinos are the most difficult to detect in the DM annihilating final states, the authors of Ref. [17] and [18] assumed that the DM annihilate solely into neutrinos. They calculated the extra-galactic and the galactic neutrino fluxes, compared them with atmospheric neutrino flux, and set an upper bound on the DM annihilation cross section $\langle\sigma v\rangle$. However, the DM may annihilate into final states other than neutrinos. In most of

the DM models there are several annihilation channels. Moreover high energy neutrinos from the DM annihilation will lead to gauge bosons bremsstrahlung [19, 20] even in the standard model (SM). The electromagnetic final states through higher-order corrections are also inevitable [21]. Therefore the assumption that DM annihilate into only neutrinos gives the most conservative bound on DM annihilation cross section.

In this paper we calculated the neutrino flux from the DM annihilations in the MW including the contributions from sub-halos by assuming that the DM annihilate into neutrinos only [17, 18]. By comparing the predicted flux with the available atmospheric neutrino measurements, we set a very strict constraint on the DM total annihilation cross section. Compared to the previous studies, in this work we utilize the angular resolution of the neutrino telescope to derive the stricter constraints. Here the massive sub-halos can be treated as the point-like sources. Based on our analysis we may observe the high energy neutrino flux provided that precise angular resolution data from ANTARES [22] and IceCube [23] is available. On the other hand if no excess flux out of atmospheric neutrino is observed, an improved upper-bound of the annihilation cross section and/or the exclusion of certain sub-halo models can be obtained.

This paper is organized as following. In Sec. II, we describe the sub-halo models according to the N-body simulation results. In Sec. III, we give the constraints on the dark matter annihilation cross section. The conclusions and discussions are given in Sec. IV.

II. GALACTIC DM DISTRIBUTION AND SUBSTRUCTURE

The current knowledge of the DM spatial distribution is mostly from the N-body simulation. Navarro et al. [24] firstly proposed a universal DM profile (referred as “NFW”). Based on their simulation in a wide range of halo mass, the density of DM can be written as [24]

$$\rho(r) = \frac{\rho_s}{(r/r_s)[1 + r/r_s]^2}, \quad (1)$$

where ρ_s and r_s are the density scale and radius parameters for a specific DM halo. Moore et al. [25] gave another profile with a more cusped inner slope compared with NFW as

$$\rho(r) = \frac{\rho_s}{(r/r_s)^{1.5}[1 + (r/r_s)^{1.5}]}. \quad (2)$$

In addition, cored profile as $\frac{\rho_s}{(1+r/r_s)[1+(r/r_s)^2]}$ [26, 27] or cuspy profile with different inner slope from NFW and Moore (e.g., [28]) were also proposed in the literature. Reed et al.

showed that even the inner slope steepens with the decrement of the halo mass, instead of a universal one [29]. All these profiles give the same behaviors $\sim r^{-3}$ at large radii, but show discrepancies in the inner region of the halo. Precise determination of the DM profile needs simulation with higher resolution and better understanding of the DM properties such as the interaction with baryonic matter. In this work we will adopt both NFW and Moore profiles for the discussion. It should be noted that the central density for NFW or Moore profile is divergent. In order to handle the singularity, a characteristic radius r_c is introduced within which the DM density is kept a constant ρ_{max} due to the balance between the annihilation rate and the in-falling rate of DM [30]. Typically we have $\rho_{max} = 10^{18} \sim 10^{19} M_\odot \text{ kpc}^{-3}$ [31].

A. Determination of the profile parameters r_s and ρ_s

Following [32], we use the virial mass M_v of the halo to determine the parameters ρ_s and r_s . For a DM halo with specified mass M_v , the virial radius r_v is defined as

$$r_v = \left(\frac{M_v}{(4\pi/3)\Delta\rho_c} \right)^{1/3}, \quad (3)$$

with the density amplifying factor over the background $\Delta \approx 200$ and the critical density of the universe $\rho_c = 139 M_\odot \text{ kpc}^{-3}$. The concentration parameter c_v (CP) is defined as

$$c_v = \frac{r_v}{r_{-2}}, \quad (4)$$

where r_{-2} refers to the radius at which $\frac{d(r^2\rho)}{dr}|_{r=r_{-2}} = 0$. It is shown that for NFW profile $r_{-2} = r_s^{nfw}$ and for Moore profile $r_{-2} = 0.63 r_s^{moore}$, so we have

$$r_s^{nfw} = \frac{r_v(M_v)}{c_v(M_v)}, \quad r_s^{moore} = \frac{r_v(M_v)}{0.63 c_v(M_v)}. \quad (5)$$

Then ρ_s can be derived just by requiring $\int \rho(r)dV = M_v$. We can see that the profile of the DM halo is fully determined provided that the $c_v - M_v$ relation is specified.

Generally the $c_v - M_v$ relation is fitted from the numerical simulation. Here we will use two toy models of Eke et al. ([33], denoted by ENS01) and Bullock et al. ([32], denoted by B01), within which the DM halo forms based on the cosmological background density field. The CP predicted in these models increases with the decrement of the halo mass.

Such behavior is understandable in the frame of hierarchy structure formation, i.e. smaller halo forms earlier when the universe is denser than today. This behavior is confirmed at the cluster scale [34, 35]. However, other studies showed agreement or disagreement with these two models, which indicate that we may not achieve the final understanding of this topic at present (see the discussion of Ref. [31]). For the current work, these models are regarded as reference ones. We use the fitted polynomial form of the simulation at $z = 0$ and extrapolate to low masses [31]:

$$\ln(c_v) = \sum_{i=0}^4 C_i \times \left[\ln \frac{M_v}{M_\odot} \right]^i, \quad (6)$$

with M_\odot the mass of the Sun and

$$C_i^{ENS01} = \{3.14, -0.018, -4.06 \times 10^{-4}, 0, 0\} \quad (7)$$

and

$$C_i^{B01} = \{4.34, -0.0384, -3.91 \times 10^{-4}, -2.2 \times 10^{-6}, -5.5 \times 10^{-7}\}. \quad (8)$$

Fig. 1 shows c_v as a function of the halo mass M_v (see also Fig. 1 of Ref. [36]). For the very low mass, it is shown that c_v becomes flat due to the fact that small objects tend to collapse at the same epoch. It should be noted that ENS01 and B01 models are for distinct halos in the universe. For the sub-halos within a host halo which is denser than the universe background, as we will discuss in this work, it is expected to be more concentrated than the distinct halos. In Ref. [32] the simulation showed the sub-halos within a host halo indeed have larger c_v than the distinct ones with the same mass. The simulation shows the c_v of subhalo has $c_v \sim M_v^{-0.3}$, which is steeper than the distinct halo ($c_v \sim M_v^{-0.13}$). In Fig. 1 we also show the extrapolated results of c_v for sub-halos with mass $10^6 \sim 10^{12} M_\odot$. The other way to deal with the sub-halo is to multiply the result for distinct one by an empirical factor (e.g., ~ 2 in Ref. [36], in the following we denote this model as $B01 \times 2$).

B. The MW halo and substructure

The mass of the MW DM halo is about $1 \sim 2 \times 10^{12} M_\odot$ determined from the rotation curve or kinematics of tracer populations such as the stars, satellite galaxies and globular clusters [37, 38, 39]. A recent work by Xue et al. showed that $M_v = (0.93 \pm 0.25) \times 10^{12} M_\odot$

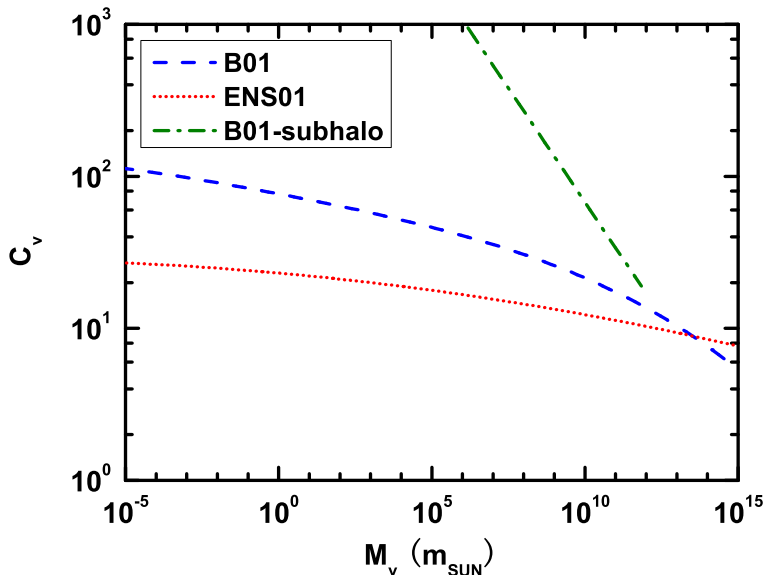


FIG. 1: Concentration parameter (CP) c_v as a function of halo mass M_v at epoch $z = 0$.

through an analysis of kinematics of a large sample of SDSS halo stars [40]. Here we adopt $M_v = 10^{12} M_\odot$ as the mass of the total MW halo. As shown below, about 10% \sim 20% of the mass will form substructures, so the mass of the smooth halo is $0.8 \sim 0.9 \times 10^{12} M_\odot$. A NFW profile is adopted for the smooth halo. Using the B01 model, we find that¹ $r_v \approx 205$ kpc, $c_v \approx 13.6$ and $\rho_\odot \approx 0.34 \text{ GeV cm}^{-3}$. This configuration of the smooth halo is fixed in the following discussion since we will focus on the substructure in the present work.

The survival of substructure in galactic halo was revealed by many simulation groups [41, 42, 43, 44, 45, 46, 47]. A recent simulation conducted by Diemand et al. showed that the self-bound substructure could even be as light as the Earth, with a huge number reaching $\sim 10^{15}$ [28]. Simulations give the number density of sub-halos an isothermal spatial distribution and a power-law mass function as

$$\frac{dN}{dM_{sub} \cdot 4\pi r^2 dr} = N_0 \left(\frac{M_{sub}}{M_{host}} \right)^{-\alpha} \frac{1}{1 + \left(\frac{r}{r_H} \right)^2}, \quad (9)$$

¹ Here $10^{12} M_\odot$ is used to calculate r_v and c_v , while the density at the solar location is scaled to match that of the mass of the smooth component is $0.85 \times 10^{12} M_\odot$.

where M_{sub} and M_{host} are the masses of sub-halo and host halo ($10^{12} M_{\odot}$ here), r_H is the core radius which usually is a fraction of the virial radius of the host halo, α is the slope of the mass function and N_0 is the normalization factor. For a galactic host halo, r_H was found to be about $0.14 r_v$ [48]. The slope α lies between 1.7 and 2.1 in various works [43, 44, 47, 49, 50, 51]. Here we adopt $\alpha = 1.9$ as in Ref. [12, 14, 36]. The mass function of Eq. (9) is thought to be held in the mass range from the minimal sub-halo with mass $\sim 10^{-6} M_{\odot}$ which is close to the free-streaming mass [28, 52, 53, 54], to the maximum one about $0.01 M_{host}$ [12]. The normalization is determined by setting the number of sub-halos with mass larger than $10^8 M_{\odot}$ is 100 [31]. Finally in the inner region of the host halo, strong tidal force tends to destroy the sub-halo and the survival number should be cut down. We employ the ‘‘tidal approximation’’ as in Ref. [12]. Under this configuration, we find that the mass fraction of substructure is about 14%.

C. Astrophysical factor of the DM annihilation

The annihilation signal of DM particles relies on two factors: the particle physical factor $W(E)$ (energy dependent) depending on the particle property of DM, and the astrophysical factor $J(\psi)$ (spatial dependent) depending on the spatial distribution of DM. The neutrino flux observed on the Earth (applicable also for γ) can be written as

$$\begin{aligned} \phi(E, \psi) &= C \times W(E) \times J(\psi) \\ &= \rho_{\odot}^2 R_{\odot} \times \frac{1}{4\pi} \frac{\langle \sigma v \rangle}{2m_{\chi}^2} \frac{dN}{dE} \times \frac{1}{\rho_{\odot}^2 R_{\odot}} \int_{LOS} \rho^2(l) dl, \end{aligned} \quad (10)$$

where $\rho_{\odot} = 0.34 \text{ GeV cm}^{-3}$ is the local DM density and $R_{\odot} = 8.5 \text{ kpc}$ is the distance of the Sun from the GC, ψ is defined as the angle between the observational direction and the GC direction relative to the observer, $\langle \sigma v \rangle$ is the average value of annihilation cross section times relative velocity, m_{χ} is the mass of DM particle, dN/dE is the production spectrum of ν per annihilation. The integral path in Eq. (10) is along the line-of-sight (LOS). To account for the contribution of substructures, we just need to replace ρ^2 in Eq. (10) by $\langle \rho^2 \rangle = \rho_{smooth}^2 + \langle \rho_{sub}^2 \rangle$ with [14]

$$\langle \rho_{sub}^2 \rangle = \int dM_{sub} \frac{dN}{dM_{sub} \cdot 4\pi r^2 dr} \left(\int_{V_{sub}} \rho_{sub}^2 dV \right). \quad (11)$$

The average astrophysical factor within a solid angle $\Delta\Omega$ (e.g., the angular resolution of

the detector) is defined as

$$J_{\Delta\Omega} = \frac{1}{\Delta\Omega} \int_{\Delta\Omega} J(\psi) d\Omega. \quad (12)$$

where $J(\psi)$ is defined in Eq. (10). In Fig. 2 we show $J(\psi)$ as a function of ψ and $J_{\Delta\Omega}$ as a function of smooth angle $\Delta\Theta$, which is the half angle of the cone centered at the direction of the GC. Here $\Delta\Omega = 2\pi(1 - \cos \Delta\Theta)$. From the figures we can see that the enhancement on $J(\psi)$ by substructures is mainly at large angle, i.e., the direction deviation from the GC. The contribution from sub-halos with Moore profile is about 8 times larger than that of NFW profile (slightly different between various concentration models). For ENS01 model the enhancement upon the smooth component is very weak, while for the best combination B01×2+Moore the boost factor can be as large as ~ 25 at the anti-GC direction. However, the enhancement of $J_{\Delta\Omega}$ is not remarkable. For the halo-average ($\Delta\Theta = 180^\circ$) the best case gives ~ 4 times boost as shown in the right bottom figure in Fig. 2.

D. DM substructure as point-like source

In the previous section the contribution from substructures is averaged over the whole MW (see Eq. (11)). It should be noted that for the few massive sub-halos this average is unreasonable. In this case, the massive sub-halo should be more appropriately treated as point-like source and may be identified by high angular resolution detector such as the IceCube. This feature can also be utilized to suppress the background.

In our work, a Monte-Carlo method is adopted to produce sub-halos with mass larger than $10^6 M_\odot$ according to the distribution function Eq. (9). For this distribution function, we find $N(> 10^6 M_\odot) \approx 6400$. In our numerical simulation, totally 50 MWs are generated, and the “tidal approximation” is adopted. For each sub-halo, we calculate the value of $J(\psi)$ and average within the cone with half angle equal to 1° . Then we count the cumulative number of sub-halos with astrophysical factor larger than a specified value, as shown in Fig. 3. The concentration models for ENS01, B01 and B01-subhalo (see Fig. 1) are adopted. We can see that the ENS01 model gives the smallest astrophysical factor, while the result from B01-subhalo model is larger by orders of magnitude than other models. From the figure we can see that the uncertainties of density distribution in sub-halos are very large. Given the particle factor of DM annihilation, we can get the number of sub-halos with flux higher than a specified value, such as the sensitivity of the detector. On the contrary, if no source

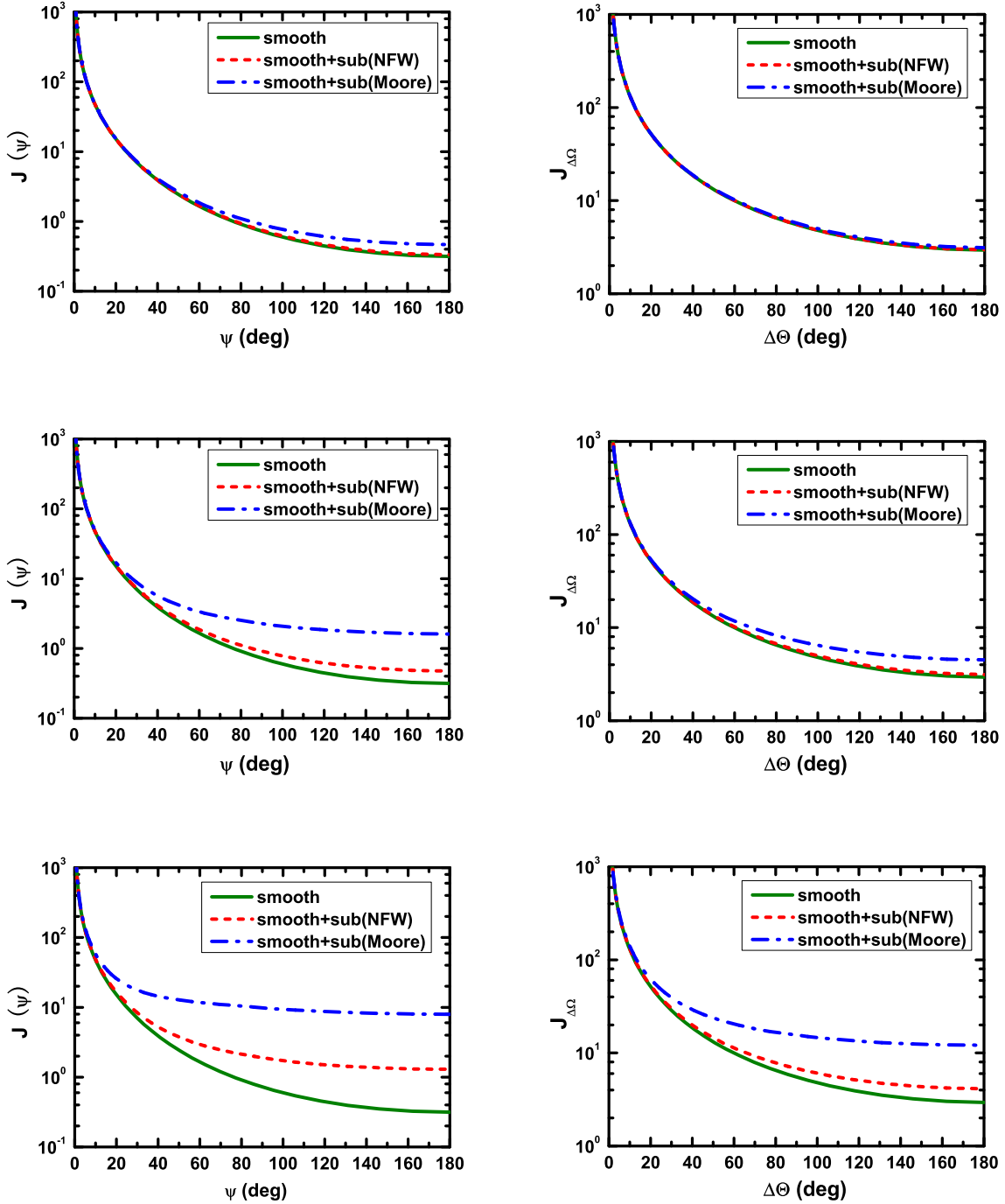


FIG. 2: $J(\psi)$ as a function of ψ (left column) and $J_{\Delta\Omega}$ as a function of smooth angle $\Delta\Theta$ —half angle of the smooth cone centered at the direction of GC (right column). In each figure the smooth (solid), smooth+sub(NFW) (dashed) and smooth+sub(Moore) (dotted) are shown. For each column, from top to bottom, the figures correspond to the concentration models as ENS01, B01 and B01 multiplying by a factor of 2, respectively.

is seen, it puts a constraint on the DM annihilation cross section [55].

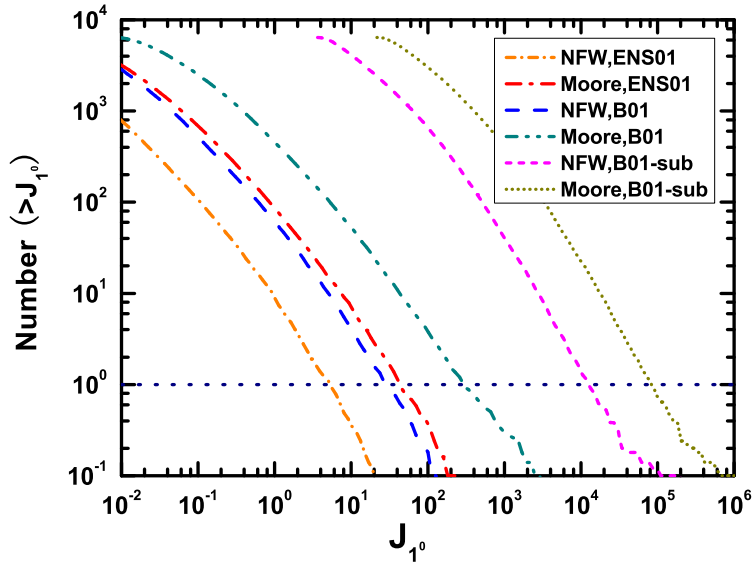


FIG. 3: Cumulative number of sub-halos whose astrophysical factor $> J_{1^\circ}$ as a function of J_{1° . The dashed horizon line corresponds to the case that only one subhalo will be observed.

III. CONSTRAINT ON DARK MATTER ANNIHILATION CROSS SECTION FROM MEASUREMENTS OF ATMOSPHERIC NEUTRINO FLUX

The atmospheric neutrino comes from hadronic interaction between cosmic ray and atmosphere around the Earth. The observed neutrino flux is consistent with theoretical prediction within the uncertainties [56, 57]. The neutrinos from the DM annihilation should not be larger than the measured flux of the neutrino. Thus this requirement gives bounds on the DM annihilation cross section provided that the astrophysical factor, as discussed in the above section, is known. Actually in the literature the constraints on the neutrino fluxes from cosmic diffuse processes and the whole MW halo have been investigated in Ref. [17, 18]. In this work, influence on neutrino flux by DM substructures will be scrutinized.

We assume that DM particles annihilate into pairs of neutrinos following Ref. [17]. The spectrum of the neutrinos per flavor is a monochromatic line with $dN_\nu/dE_\nu = \frac{2}{3}\delta(E_\nu - m_\chi)$,

where m_χ is the mass of the DM particle. All neutrino flavors are equally populated and the neutrino and anti-neutrino are added together. We require that the average neutrino flux from DM annihilation should not exceed the average atmospheric neutrino flux, which is taken from [58].

We first consider the neutrino flux averaged over all directions with smooth and sub-halo contributions. As shown by the left column in Fig. 2, the sub-halo contribution to the neutrino flux is insensitive to the direction [12], while the smooth contribution can vary by several orders of magnitude for GC and anti-GC directions. The sub-halo contribution in anti-GC direction is larger than that of the smooth one, but smaller in GC direction. In other words, the neutrinos from anti-GC direction are mainly from sub-halo DM annihilation.

Second, we investigate the effects on the neutrino flux from DM sub-halo contribution. Massive sub-halo is more appropriately treated as point-like source, as discussed above. We take smaller angle cone to calculate the neutrino flux from such single sub-halo and the atmospheric neutrino separately. The average neutrino flux from sub-halo in this cone is required not to exceed the atmospheric neutrino flux. Combined with the input astrophysical factor, we can set bounds on the DM annihilation cross section. This approach is obviously based on the excellent angular resolution of the neutrino telescope. The angular resolution of Super-Kamiokande is $\delta\theta(E) \simeq 30^\circ \times \sqrt{GeV/E}$ [57]. For $E > 100GeV$ neutrino, the angular resolution can reach about 3° for Super-Kamiokande, while 1° for IceCube [23]. In our evaluation we adopt a 1° half-angle cone for IceCube. Note that for IceCube, the candidate source should be in the northern sky, and its threshold energy is $50GeV$ [23].

In order to obtain the constraint on the DM annihilation cross section, we must input the astrophysical factor. We use average neutrino flux in a cone $\phi_{\Delta\Omega}$ by simply replacing $J(\psi)$ with $J_{\Delta\Omega}$ in Eq. (10). Since the DM induced neutrino is sharply peaked, we average neutrino flux within the energy bin around $E_\nu = m_\chi$ to compare with the atmospheric neutrinos. And the energy bin width is taken as $\Delta \log_{10} E = 0.3$ within the energy resolution limits of the neutrino detectors Super-Kamiokande [15, 57] and IceCube [23]. The $J_{\Delta\Omega}$ used in sub-halo point source is taken from Fig. 3 when cumulative number equals to one. Based on the astrophysical factor input this way, the derived annihilation cross section gives the sensitivity that IceCube may find at least one sub-halo. $J_{\Delta\Omega}$ for different sub-halo profiles and concentration models are given in Table. I.

From Table I we can see that $J_{\Delta\Omega}$ is 3.0 for the smooth case. The sub-halo contribution

	Halo average		Point-like		
	smooth	smooth + subhalo	ENS01	B01	B01-subhalo
NFW	3.0	4.1	5.3	28.9	12763.7
Moore	—	12.1	43.3	276.3	82110.2

TABLE I: $J_{\Delta\Omega}$ for different sub-halo profiles and concentration models. The values listed here correspond to the cumulative number equal to 1 as shown in Fig. 3. The smooth contribution to $J_{\Delta\Omega}$ is fixed to be NFW profile. 'Halo average' means averaging contributions over the whole MW halo. For the sub-halo contributions we choose the concentration model of $B01 \times 2$, as shown in the bottom-right figure in Fig. 2. ENS01, B01 and B01subhalo represent different concentration models when considering DM substructure as point-like sources. For point-like sub-halos, $J_{\Delta\Omega}$ is averaged in a 1° half-angle cone around the center of the sub-halo.

with Moore profile is 9.1, while only 1.1 for NFW profile. If one averages the contributions over the whole sky, the sub-halo contribution can enhance the neutrino flux slightly. As shown in Fig. 2, the enhancement of sub-halo is large at the anti-GC direction which can reach about $100 \sim 1000$, but the enhancement at the GC direction is small. Note that the flux from the GC is much larger than that from the anti-GC, it is natural to expect the *averaging* sub-halo contribution should not be significant. Therefore the point-like sub-halo should be naturally more important, as shown in Table I. For the different concentration model ENS01, B01 and B01subhalo, $J_{\Delta\Omega}$ is much larger than the average contribution, though the uncertainty is very large. The numbers in different concentration models can be understood from Fig. 1, which indicates that the large c_v corresponds to the large $J_{\Delta\Omega}$. Virial radius r_v defined in Eq. 4 is the boundary that gravitational force can sustain itself, and it is only related to virial mass M_v but not the mass distribution. The density profiles with NFW or Moore distribution behave both like r^{-3} at large radii and r^{-1} or $r^{-1.5}$ at small radii separately. The radius r_{-2} is a measure of the density profile $\rho(r)$, namely the dark matter distributes mainly within the region $r < r_{-2}$. Thus larger c_v means more dark matter concentrating in the sub-halo center, which results in a larger $J_{\Delta\Omega}$.

Once the astrophysical factor is known, bounds on the dark matter annihilation cross section $\langle\sigma v\rangle$ can be derived by requiring the DM induced neutrino flux less than the measured ones. In Fig. 4 and Fig. 5, the upper bounds on $\langle\sigma v\rangle$ are plotted for two DM profiles. Also

shown in the figures is $\langle\sigma v\rangle$ for the natural scale of dark matter. The upper solid line correspond to the constraints from 180° half-angle cone averaging contributions. The other lines represent the sub-halo point source with 1° resolution from the IceCube. The dashed, dash-dotted and short-dashed lines are plotted with different concentration models. The constraints from the whole halo average are slightly improved compared with the smooth case in Refs. [17, 18]. For the sub-halo as the point source, the constraints are significantly improved. Moreover the upper bounds of $\langle\sigma v\rangle$ are about $10^{-23} \sim 10^{-24} \text{ cm}^3 \text{ s}^{-1}$ for B01 model, and can even reach $\sim 10^{-26} \text{ cm}^3 \text{ s}^{-1}$ for B01-subhalo model. Such bound is even lower than $\langle\sigma v\rangle$ for the natural scale which can induce the correct relic density of DM.

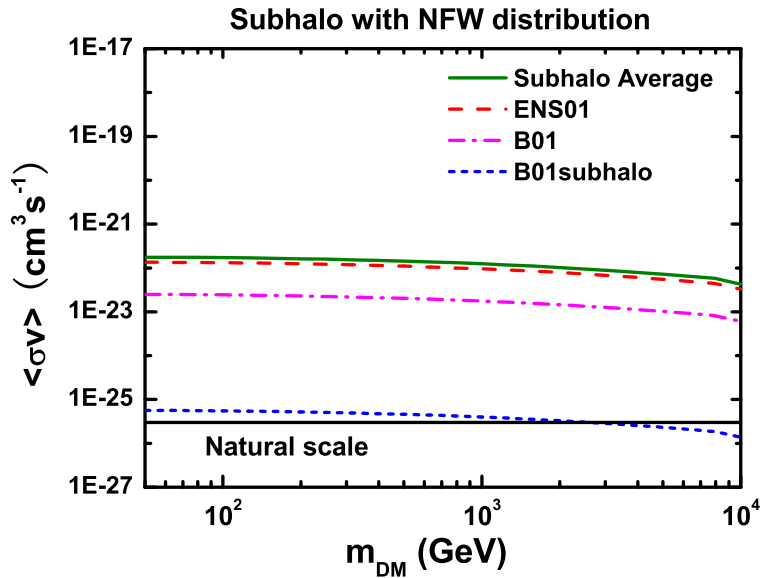


FIG. 4: The upper bounds on the DM annihilation cross section $\langle\sigma v\rangle$ as a function of dark matter mass with NFW subhalo profile. The upper solid lines represent the constraints from 180° half-angle cone average. The other lines represent constraints from sub-halo point source with 1° resolution from the IceCube. The dashed, dash-dotted and short-dashed lines are plotted for different concentration models. The lower solid line corresponds to $\langle\sigma v\rangle \sim 3 \times 10^{-26} \text{ cm}^3 \text{ s}^{-1}$ for the natural scale to produce the correct thermal relic density.

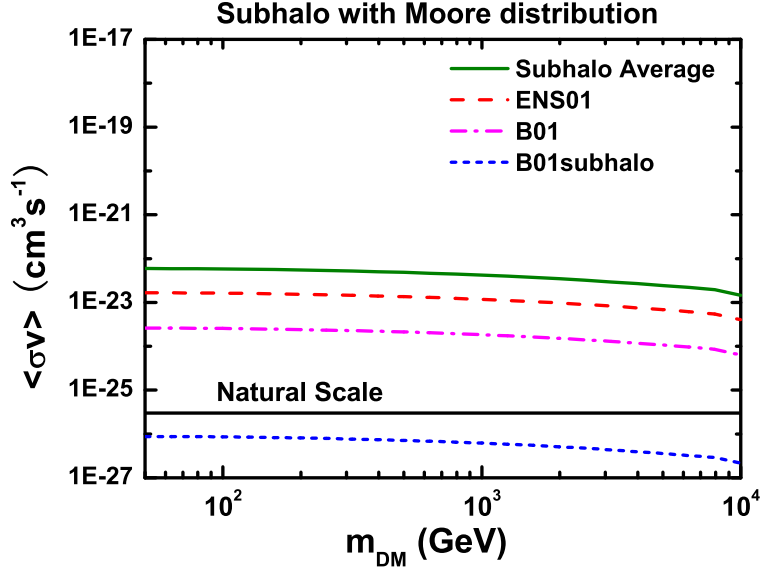


FIG. 5: Same with Fig. 4 but with Moore subhalo profile.

IV. CONCLUSIONS AND DISCUSSIONS

In this paper, by requiring the DM induced neutrino flux less than the measured ones, we give the improved upper bounds on the DM annihilation cross section $\langle\sigma v\rangle$ with the DM substructure effects included. Here we assume the DM particles annihilate into neutrinos solely following the previous works. The observed neutrino flux depends on the particle physical and astrophysical factors. Thus we first investigate the astrophysical factor. Several different DM profiles and sub-halo concentration models are adopted based on the numerical simulations. Our studies show that at the anti-GC direction, the enhancement factor of sub-halos for B01 \times 2 model is about 3 and 25 for NFW and Moore profiles respectively. While the whole-sky average (*halo average*, with cone half-angle 180°) does not have prominent enhancement. The best case of our adopted models is only ~ 4 times larger than the smooth ones (see bottom-right figure in Fig. 2). If we take the 30° angular average (*halo angular* in Ref. [18]), there is almost no enhancement, as can be seen in Fig. 2. This is because the enhancement from sub-halos is spatially dependent on the MW halo, instead of a universal one [13]. On one hand, the smooth component increases more rapidly and dominates the annihilation flux near the GC; on the other hand, the tidal disruption on sub-halos is most

effective close to the GC. Thus the effect of substructures is not significant near the GC. In the cases of *halo average* and *halo angular*, the GC contributions are included and play a dominant role in the total flux, therefore no remarkable enhancement from sub-halos is found.

In this paper we emphasize the important role of the massive sub-halos (e.g., $M_{sub} > 10^6 M_\odot$). Since the number of massive sub-halo is small, it should be regarded as the point-like source. For the massive sub-halos, the high angular resolution of neutrino detector can be utilized to suppress the atmospheric neutrino background, thus the constraints on $\langle\sigma v\rangle$ are expected to be improved. The angular resolution $\sim 1^\circ$ for energy greater than 50 GeV of the forthcoming experiment IceCube is employed ². The neutrino signal flux in a cone with half-angle 1° is calculated and compared with the atmospheric background in the same cone. We found that the constraints on $\langle\sigma v\rangle$ are indeed improved significantly. Note that the constraints are model-dependent. For the moderate case B01+NFW, we find the upper bound of $\langle\sigma v\rangle$ is about $10^{-23} \text{ cm}^3 \text{ s}^{-1}$. While for the concentration model B01-subhalo, the bound can reach $10^{-26} \text{ cm}^3 \text{ s}^{-1}$, which is even lower than $\langle\sigma v\rangle$ for the natural scale which can induce the correct relic density of DM.

It should be noted that DM can annihilate into final states other than neutrinos. Thus the assumption that DM annihilates into only neutrinos gives the most conservative bound on the DM annihilation cross section and is independent of the particle properties of DM particle.

Neutrinos are thought to be an important complementary particles for DM indirect searches besides γ -rays and charged anti-particles. It is shown that the detectability of γ -rays from DM sub-halos on GLAST is optimistic [59]. The effects of subhalos on positrons [60, 61] and antiprotons [31] are also investigated. The combination and cross check of different kinds of signals will be very crucial to identify the DM sources and investigate the properties of DM particles.

² For Super-Kamiokande, the resolution angle is $\sim 3^\circ$ for $E > 100 \text{ GeV}$ and the background is 9 times greater.

V. ACKNOWLEDGEMENTS

This work was supported in part by the Natural Sciences Foundation of China (Nos. 10775001, 10635030, 10575111, 10773011), by the trans-century fund of Chinese Ministry of Education, and by the Chinese Academy of Sciences under the grant No. KJ CX3-SYW-N2.

-
- [1] G. Jungman, M. Kamionkowski and K. Griest, *Phys. Rept.* **267**, 195 (1996).
 - [2] K. G. Begeman, A. H. Broeils and R. H. Sanders, *Mon. Not. Roy. Astron. Soc.* **249**, 523 (1991).
 - [3] M. Persic, P. Salucci and F. Stel, *Mon. Not. Roy. Astron. Soc.* **281**, 27 (1996).
 - [4] J. A. Tyson and P. Fischer, *Astrophys. J.* **446** 55 (1995).
 - [5] S. D. M. White, J. F. Navarro, A. E. Evrard and C. S. Frenk, *Nature* **366**, 429 (1993).
 - [6] P. J. E. Peebles, *Physical Cosmology* (Princeton: Princeton University Press) (1971).
 - [7] D. N. Spergel *et al.* [WMAP Collaboration], *Astrophys. J. Suppl.* **148**, 175 (2003).
 - [8] G. Hinshaw *et al.* [WMAP Collaboration], arXiv:0803.0732 [astro-ph].
 - [9] G. Bertone, D. Hooper and J. Silk, *Phys. Rept.* **405**, 279 (2005).
 - [10] J. Liu, P. f. Yin and S. h. Zhu, *Phys. Rev. D* **77**, 115014 (2008) and references therein.
 - [11] P. Gondolo and J. Silk, *Phys. Rev. Lett.* **83**, 1719 (1999).
 - [12] X. J. Bi, *Nucl. Phys. B* **741**, 83 (2006).
 - [13] X. J. Bi, J. Zhang, Q. Yuan, J. L. Zhang and H. Zhao, arXiv:astro-ph/0611783.
 - [14] Q. Yuan and X. J. Bi, *JCAP* **0705**, 001 (2007).
 - [15] S. Desai *et al.* [Super-Kamiokande Collaboration], *Phys. Rev. D* **70**, 083523 (2004) [Erratum-*ibid.* *D* **70**, 109901 (2004)].
 - [16] J. Ahrens *et al.* [AMANDA Collaboration], *Nucl. Instrum. Meth. A* **524** (2004) 169; M. Ackermann *et al.* [The AMANDA Collaboration], *Phys. Rev. D* **71**, 077102 (2005).
 - [17] J. F. Beacom, N. F. Bell and G. D. Mack, *Phys. Rev. Lett.* **99**, 231301 (2007).
 - [18] H. Yuksel, S. Horiuchi, J. F. Beacom and S. Ando, *Phys. Rev. D* **76**, 123506 (2007).
 - [19] M. Kachelriess and P. D. Serpico, *Phys. Rev. D* **76**, 063516 (2007).
 - [20] N. F. Bell, J. B. Dent, T. D. Jacques and T. J. Weiler, arXiv:0805.3423 [hep-ph].
 - [21] J. B. Dent, R. J. Scherrer and T. J. Weiler, arXiv:0806.0370 [astro-ph].

- [22] T. Pradier and f. t. A. Collaboration, arXiv:0805.2545 [astro-ph].
- [23] J. Ahrens *et al.* [IceCube Collaboration], *Astropart. Phys.* **20**, 507 (2004).
- [24] J. F. Navarro, C. S. Frenk and S. D. M. White, *Astrophys. J.* **490**, 493 (1997).
- [25] B. Moore, F. Governato, T. Quinn, J. Stadel and G. Lake, *Astrophys. J.* **499**, L5 (1998).
- [26] A. Burkert, *IAU Symp.* **171**, 175 (1996) [*Astrophys. J.* **447**, L25 (1995)].
- [27] P. Salucci and A. Burkert, *Astrophys. J.* **537**, L9 (2000).
- [28] J. Diemand, B. Moore and J. Stadel, *Nature* **433**, 389 (2005).
- [29] D. Reed *et al.*, *Mon. Not. Roy. Astron. Soc.* **357**, 82 (2005).
- [30] V. S. Berezinsky, A. V. Gurevich and K. P. Zybin, *Phys. Lett. B* **294**, 221 (1992).
- [31] J. Lavalley, Q. Yuan, D. Maurin and X. J. Bi, *Astron. Astrophys.* **479**, 427 (2008).
- [32] J. S. Bullock *et al.*, *Mon. Not. Roy. Astron. Soc.* **321**, 559 (2001).
- [33] V. R. Eke, J. F. Navarro and M. Steinmetz, *Astrophys. J.* **554**, 114 (2001).
- [34] D. A. Buote, F. Gastaldello, P. J. Humphrey, L. Zappacosta, J. S. Bullock, F. Brighenti and W. G. Mathews, *Astrophys. J.* **664**, 123 (2007).
- [35] J. M. Comerford and P. Natarajan, *Mon. Not. Roy. Astron. Soc.* **379**, 190 (2007).
- [36] S. Colafrancesco, S. Profumo and P. Ullio, *Astron. Astrophys.* **455**, 21 (2006).
- [37] M. I. Wilkinson and N. W. Evans, *Mon. Not. Roy. Astron. Soc.* **310**, 645 (1999).
- [38] T. Sakamoto, M. Chiba and T. C. Beers, *Astron. Astrophys.* **397**, 899 (2003).
- [39] M. C. Smith *et al.*, *Mon. Not. Roy. Astron. Soc.* **379**, 755 (2007).
- [40] X. X. Xue *et al.*, arXiv:0801.1232 [astro-ph].
- [41] G. Tormen, A. Diaferio and D. Syer, *Mon. Not. Roy. Astron. Soc.* **299**, 728 (1998).
- [42] A. A. Klypin, S. Gottlober and A. V. Kravtsov, *Astrophys. J.* **516**, 530 (1999).
- [43] B. Moore, S. Ghigna, F. Governato, G. Lake, T. Quinn, J. Stadel and P. Tozzi, *Astrophys. J.* **524** (1999) L19.
- [44] S. Ghigna, B. Moore, F. Governato, G. Lake, T. Quinn and J. Stadel, *Astrophys. J.* **544**, 616 (2000).
- [45] V. Springel, S. D. M. White, G. Tormen and G. Kauffmann, *Mon. Not. Roy. Astron. Soc.* **328**, 726 (2001).
- [46] A. R. Zentner and J. S. Bullock, *Astrophys. J.* **598**, 49 (2003).
- [47] G. De Lucia *et al.*, *Mon. Not. Roy. Astron. Soc.* **348**, 333 (2004).
- [48] J. Diemand, B. Moore and J. Stadel, *Mon. Not. Roy. Astron. Soc.* **352**, 535 (2004).

- [49] A. Helmi, S. D. M. White and V. Springel, *Phys. Rev. D* **66**, 063502 (2002).
- [50] L. Gao, S. D. M. White, A. Jenkins, F. Stoehr and V. Springel, *Mon. Not. Roy. Astron. Soc.* **355** (2004) 819.
- [51] L. Shaw, J. Weller, J. P. Ostriker and P. Bode, *Astrophys. J.* **646**, 815 (2006).
- [52] S. Hofmann, D. J. Schwarz and H. Stoecker, *Phys. Rev. D* **64**, 083507 (2001).
- [53] X. l. Chen, M. Kamionkowski and X. m. Zhang, *Phys. Rev. D* **64**, 021302 (2001).
- [54] A. M. Green, S. Hofmann and D. J. Schwarz, *JCAP* **0508**, 003 (2005).
- [55] X. J. Bi, *Phys. Rev. D* **76**, 123511 (2007).
- [56] J. Ahrens *et al.* [AMANDA Collaboration], *Phys. Rev. D* **66**, 012005 (2002).
- [57] Y. Ashie *et al.* [Super-Kamiokande Collaboration], *Phys. Rev. D* **71**, 112005 (2005).
- [58] M. Honda, T. Kajita, K. Kasahara, S. Midorikawa and T. Sanuki, *Phys. Rev. D* **75**, 043006 (2007).
- [59] M. Kuhlen, J. Diemand and P. Madau, arXiv:0805.4416 [astro-ph].
- [60] D. T. Cumberbatch and J. Silk, *Mon. Not. Roy. Astron. Soc.* **374**, 455 (2007).
- [61] J. Lavalley, J. Pochon, P. Salati and R. Taillet, *Astron. Astrophys.* **462**, 827 (2007).